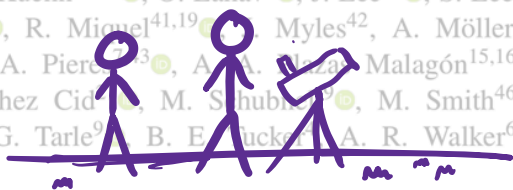




# Exploding stars show us that time slows down in the distant Universe!

Ryan M. T. White<sup>1\*</sup>, Tamara M. Davis<sup>1</sup>, Geraint F. Lewis<sup>2</sup>, Christopher Lidman<sup>3,4</sup>, Paul Sherson<sup>5</sup>, T. M. C. Abbott<sup>6</sup>, M. Aguena<sup>7</sup>, S. Allam<sup>8</sup>, F. Andrade-Oliveira<sup>9</sup>, J. Asorey<sup>10</sup>, D. Bacon<sup>11</sup>, S. Boca<sup>12</sup>, D. Brooks<sup>5</sup>, D. Brout<sup>13</sup>, E. Buckley-Geer<sup>14,8</sup>, D. L. Burke<sup>15,16</sup>, A. Carnero Rosell<sup>17,7</sup>, D. Carroll<sup>18</sup>, J. Carretero<sup>19</sup>, L. N. da Costa<sup>7</sup>, M. E. S. Pereira<sup>20</sup>, J. De Vicente<sup>21</sup>, S. Deniz<sup>22</sup>, H. T. Diehl<sup>8</sup>, S. Everett<sup>23</sup>, I. Ferrero<sup>24</sup>, B. Flaugher<sup>8</sup>, J. Frieman<sup>8,25</sup>, I. Gallego-Ordoñez<sup>6</sup>, E. Gaztanaga<sup>27,11,28</sup>, G. Giannini<sup>19,25</sup>, K. Glazebrook<sup>29</sup>, R. A. Hild<sup>30</sup>, S. R. Hinton<sup>1</sup>, D. L. Hollowood<sup>32</sup>, K. Honscheid<sup>33,34</sup>, D. Jaramillo<sup>3</sup>, R. Kessler<sup>14,25</sup>, K. Kuehn<sup>35,36</sup>, O. Lahav<sup>5</sup>, J. Lee<sup>37</sup>, S. Lee<sup>23</sup>, M. Lima<sup>38,7</sup>, J. L. Marshall<sup>39</sup>, I. M. Martínez<sup>40</sup>, R. Miquel<sup>41,19</sup>, Myles<sup>42</sup>, A. Möller<sup>29</sup>, R. C. Nichol<sup>11</sup>, R. O’Gando<sup>43</sup>, A. Palmese<sup>44</sup>, A. Pieres<sup>13</sup>, A. Plaza<sup>15,16</sup>, Malagón<sup>15,16</sup>, A. K. Romer<sup>45</sup>, M. Sako<sup>37</sup>, E. Sanchez<sup>21</sup>, D. Sanchez Cid<sup>2</sup>, M. Shubik<sup>5</sup>, M. Smith<sup>46</sup>, E. Suchyta<sup>47</sup>, M. Sullivan<sup>46</sup>, B. O. Sánchez<sup>48,49</sup>, G. Tarle<sup>9</sup>, B. E. Tucker<sup>1</sup>, A. R. Walker<sup>6</sup>, N. Weaverdyck<sup>50,51</sup>, and P. Wiseman<sup>46</sup>,



(DES Collaboration)

Affiliations are listed at the end of the paper.



So many people from so many places that we had to put the places at the end of the paper!

Accepted XXX. Received YYY; in original form ZZZ

## Here's the tl;dr...

We present a precise measurement of cosmological time dilation using the light curves of 1504 type Ia supernovae from the Dark Energy Survey spanning a redshift range  $0.1 \lesssim z \lesssim 1.2$ . We find that the width of supernova light curves is proportional to  $(1+z)^b$ , where  $b = 1.005 \pm 0.005$  (stat)  $\pm 0.010$  (sys). We use this to measure the time dilation of the supernovae, which are emitted with a consistent duration  $\Delta t_{\text{em}}$ , and parameterising the observed duration as  $\Delta t_{\text{obs}} = \Delta t_{\text{em}}(1+z)^b$ , we fit for the form of time dilation using two methods. Firstly, we find that a power law of  $b < 1$  minimises the flux scatter in stacked subsamples of light curves with different redshifts. Secondly, we use a Bayesian approach to directly compare the observed light curves with simulated ones with observed bandpasses matching that of the target light curve and find  $b = 1.005 \pm 0.005$  (stat)  $\pm 0.010$  (sys). Thanks to the large number of supernovae and large redshift range of the sample, this analysis gives the most precise measurement of cosmological time dilation to date. Our results are consistent with the prediction of general relativity, and provide the most stringent test of the theory to date. This is the most precise detection of cosmological time dilation yet.

## Here's the background:

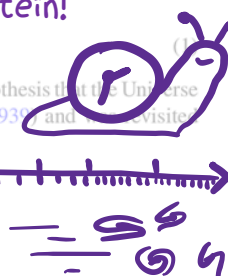
Time dilation is a fundamental implication of Einstein's theory of relativity. The time interval between two events in an inertial frame of reference is  $\Delta t_{\text{obs}} = \Delta t_{\text{em}}(1+z)$ , where  $\Delta t_{\text{em}}$  is the duration of an event in its rest frame. At  $z=0$ ,  $\Delta t_{\text{obs}} = \Delta t_{\text{em}}$ , but as  $z$  increases, the time interval between events increases. This is known as **Cosmological time dilation**.

**\*another\* prediction that can be traced back to Einstein!**

$$\Delta t_{\text{obs}} = \Delta t_{\text{em}}(1+z).$$

The idea of using time dilation to test the hypothesis that the Universe is expanding dates back as far as Wilson (1939) and has been revisited by Rust (1974).

E-mail:ryan.white@uq.edu.au  
The Authors



What we're looking for in the paper isn't a new idea; using exploding stars, supernovae, as clocks was proposed 85 years ago! Lots of people have used these and other transient light sources to quantify time dilation before...

To avoid degeneracy between the natural variation of light-curve

width and time dilation, Foley et al. (2005) and Blondin et al. (2008) observed time dilation in the evolution of spectra of high-z Type Ia supernovae (SNe Ia). The former found inconsistency with the static-universe model, finding  $b = 0.97 \pm 0.10$ . Most recently, Lewis & Brewer (2023) inferred  $b = 0.97 \pm 0.09$  using the variability of 190 quasars out to  $z \sim 4$ . Despite these successes, there remains continued discussion of hybrid or static-universe models such as Tired Light (Zwicky 1929; Gupta 2023) that do not predict expansion-induced time dilation.

In this study, we measure cosmological time dilation using SNe Ia from the full 5-year sample released by the Dark Energy Survey (DES) (DES Collaboration et al. 2024), which contains  $\sim 1500$  SNe Ia spanning the redshift range  $z = 0.05$ – $1.5$ . This is significantly larger and higher redshift than any sample of supernovae previously used for a time-dilation measurement. Such a large sample of SNe Ia is important for the first time-dilation measurement with the most statistical power. It is the ideal regime to robustly identify time dilation. Over half the DES sample (54%) have redshifts greater than  $z = 1$ , while 37% in the previous gold-standard Pantheon+sample (Bautista 2019) and 37% in the Goldhaber analysis (Goldhaber 2001). Therefore the DES sample is likely to have a much wider redshift distribution than 1.5 times longer than their rest frame durations (up to 2.2 times longer for those at  $z \sim 1.2$ ). This means their time dilation signal should be significantly larger than the intrinsic width variation expected due to SNe Ia diversity in their subtypes.

We test the model that time dilation occurs according to,

$$\Delta t_{\text{obs}} = \Delta t_{\text{em}}(1+z)^b. \quad (2)$$

If Type Ia supernovae are the result of white dwarf stars exploding, then the time dilation signal should be zero. If time dilation occurs we should find  $b = 0$ . These white dwarf stars are the super-compact remnant cores of stars that have shed their outer layers – kind of like the skeleton left over after we die. Some of

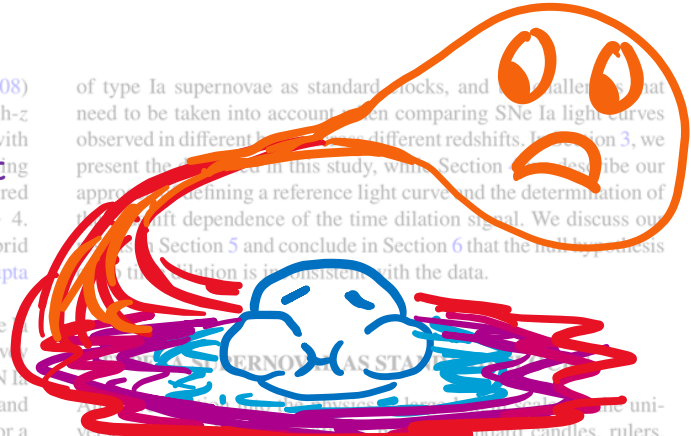
(i) Firstly, we simply take all the light curves, divide their time axes by  $(1+z)^b$  (so that they are all at the same redshift) and the value of  $b$  that minimises the flux scatter.

(ii) Secondly, we stack the individual light curves and stack them to define a ‘data-driven SN Ia reference light curve’. Then for each individual SNe Ia we measure the observed light curve width (or ‘width’ in the literature) for different values of  $w$ . The result would be  $w = (1+z)$  corresponding to  $b = 1$ .

The first method is entirely data-driven and has no time-dilation assumption. In the second method because we compute we create the stacked reference by dividing the time axis of the light curves by  $(1+z)$ . This method therefore includes an assumption of time-dilation  $w = (1+z)$ . Since they all these similar stars explode at this same critical mass, Type Ia supernovae all look pretty much the same no matter where they are!

This paper is arranged as follows. In Section 2 we discuss the use

of type Ia supernovae as standard candles, and the challenges that need to be taken into account when comparing SNe Ia light curves observed in different bands at different redshifts. In Section 3, we present the data used in this study, while Section 4 describe our approach of defining a reference light curve and the determination of the redshift dependence of the time dilation signal. We discuss our results in Section 5 and conclude in Section 6 that the null hypothesis that time dilation is inconsistent with the data.

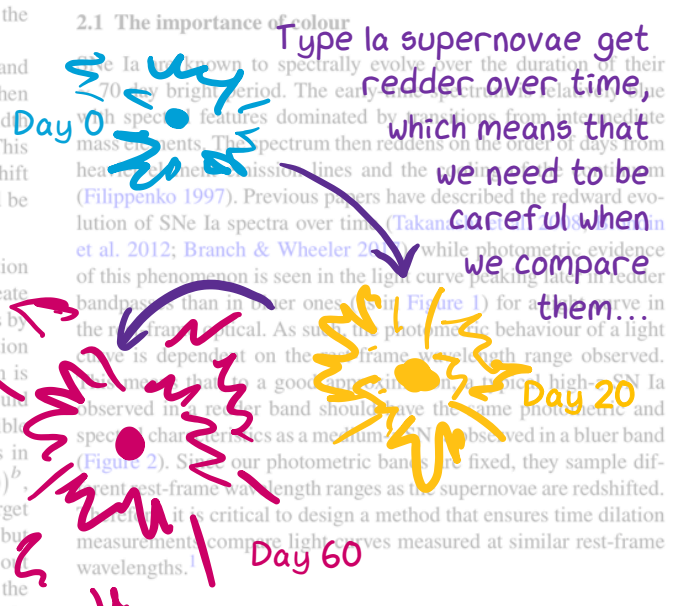


It's important to use the most distant supernovae possible for these types of studies. The further away a supernova is, the stronger the time dilation signal! This lets us find the signal amongst the noise.

We want to be really sure about how much time dilation there is as we correct for this in cosmological analyses.

The presence of a time dilation signal in SNe Ia data tests the general relativistic prediction of an expanding universe having a factor of  $(1+z)^b$  time dilation (Riess et al. 2008). This signal needs to be corrected for in supernova cosmology analyses (Taubenberger & Scolnic 2019; Scolnic et al. 2019). Accurately quantifying the effect of time dilation is foundational to our cosmological model, especially considering the continued discussion of hybrid or static-universe models such as Tired Light (Zwicky 1929; Gupta 2023) that do not predict expansion-induced time dilation.

## 2.1 The importance of colour



Type Ia supernovae get redder over time, which means that we need to be careful when we compare them... Day 0 Day 20 Day 60

Type Ia are known to spectrally evolve over the duration of their 70-day bright period. The early spectrum is relatively blue with spectral features dominated by transitions from intermediate mass elements. The spectrum then reddens on the order of days from heading towards emission lines and the peak of the spectrum (Filippenko 1997). Previous papers have described the redward evolution of SNe Ia spectra over time (Takanishi et al. 2008; Marin et al. 2012; Branch & Wheeler 2014) while photometric evidence of this phenomenon is seen in the light curve peaking later in redder bandpasses than in bluer ones (in Figure 1) for a source in the redshift range. As such, the photometric behaviour of a light curve is dependent on the rest-frame wavelength range observed. It is therefore important that a good approximation to a typical high-z SN Ia observed in a redder band should have the same photometric and spectral characteristics as a medium-z SN Ia observed in a bluer band (Figure 2). Since our photometric bands are fixed, they sample different rest-frame wavelength ranges as the supernovae are redshifted. Therefore, it is critical to design a method that ensures time dilation measurements compare light curves measured at similar rest-frame wavelengths.

<sup>1</sup> A note on language: The phrase ‘rest-frame’ wavelengths arises from the usual assumption that redshifts are due to recession velocities. The fact red-

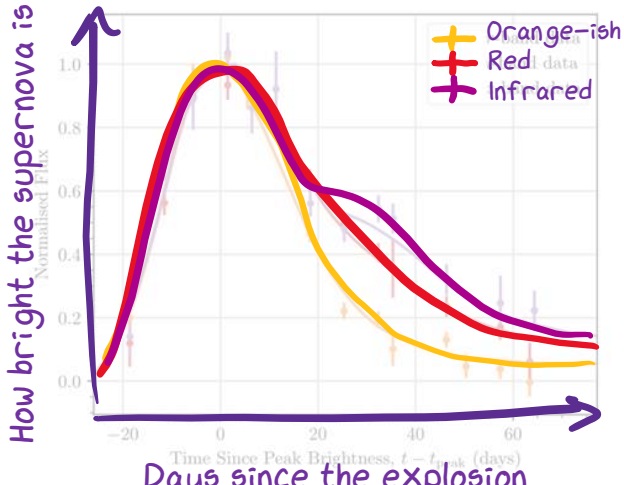


Figure 1. The normalised (in flux) light curves of a SN Ia at  $z = 0.4754$  show intrinsically broader light curves at redder wavelengths that tend to peak later (days) in the optical regime (observed across涌涌 dataset). The x-axis represents time in the observer frame and SALT3 model fits (solid lines) are overlaid on the data in each band.

**This is what our data looks like! We have 'light curves' of 1504 unique supernovae, in multiple colours**

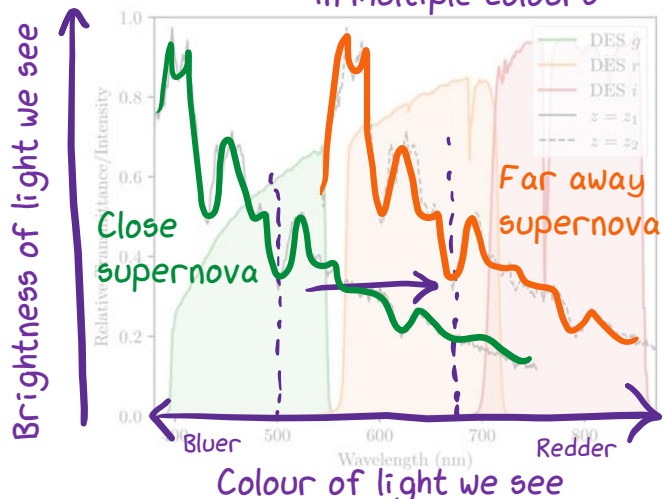


Figure 2. For a supernova at redshift  $z_1$  observed in a given filter, there exists a higher redshift  $z_2 > z_1$  such that another supernova at  $z_2$  observed in a filter with a shorter wavelength has a higher flux. This is because the light is blueshifted as the nearer supernova. We show here the spectrum of SN2001V (Matheson et al. 2008) with the transmission curves of the DES filters from Abbott et al. (2018) Fig. 1. The expanding Universe makes distant blue light appear red to us – we call this ‘redshift’. This plot shows that the colour spectrum of a supernova that’s far away is redshifted compared to one that’s close by

shifts occur is not in question here (so it is fine to use  $(1+z)$  to calculate matching rest-frame wavelengths, and this contains no time-dilation assumption). The question is whether that redshift arises due to a recession velocity, which would also cause time-dilation.

Type Ia supernovae aren’t actually as consistent as I’ve been letting on, but they do average out nicely! Some supernovae are intrinsically brighter than others and so they have ‘wider’ light curves, meaning they effectively explode for a longer duration. On the plot to the left, one of these special supernovae would be a bit taller and a bit wider!

As long as there is a representative sample of the entire population of Type Ia supernovae, the simple analysis will use time-dilation without bias. However, Malmquist bias can influence this since brighter supernovae have wider light curves. If faint supernovae are under-represented at high-redshifts one might expect a slight bias toward a higher inferred time dilation at high-redshift (getting wider by  $\sim 3\%$  between  $0 < z < 1.4$ ). Even though we don’t see this drift in the DES-SN16 sample (see Fig. A2), we quantify the possible effect in Fig. A3. We then correct for time-dilation in Appendix A and find it to be small.

**This has the same effect as time dilation and this makes our analysis a bit trickier. Luckily, the Dark Energy Survey found so many supernovae of all types that we don’t need to correct for this; it all averages out. Even if it didn’t average out, this effect is not as strong as the time dilation.**

### What data do we have?



We analyse the data from the DES Type Ia supernovae in the Dark Energy Survey (DES) and the Dark Energy Camera (DECam) at the 4m Blanco Inter-American Observatory (Isla de la Plata, Chile). We use the photometric redshifts and absolute magnitudes of the identified SN candidates and accurate redshifts in the spectroscopic sample. We also use the two colour bands available in each filter to estimate the peak flux of each SN candidate. We use these fits to estimate the peak flux of each supernova in each filter. We then use these flux values to calculate the time relative to the  $R$ -band maximum in the SALT3 fit for each light curve. This is also used to define the nine-band peak brightness measurement in SALT3. We then use this to search the SALT supernova information.

We performed an initial quality cut on the sample of 1535 SNe Ia, where we removed any that had a PROB1a > 0.6 as classified with SuperNNova (Möller & de Boisséson 2020; Möller et al. 2022; Tumlinson et al. 2022). This kept the number of usable light curves at 1504. We then removed possible type II supernova contaminants. We removed individual data points from each light curve that had an error on the flux value (FLUXCALERR for the flux value FLUXCAL) greater than 20; this was done to restrict our fitting to the highest quality observations, particularly cutting those with very low signal-to-noise at

<sup>2</sup> FLUXCALERR is the Poisson error on FLUXCAL, which is the variable used for flux in SNANA corresponding to mag = 27.5 + 5 log10(FLUXCAL)

A long time ago in  
a galaxy far, far  
away...

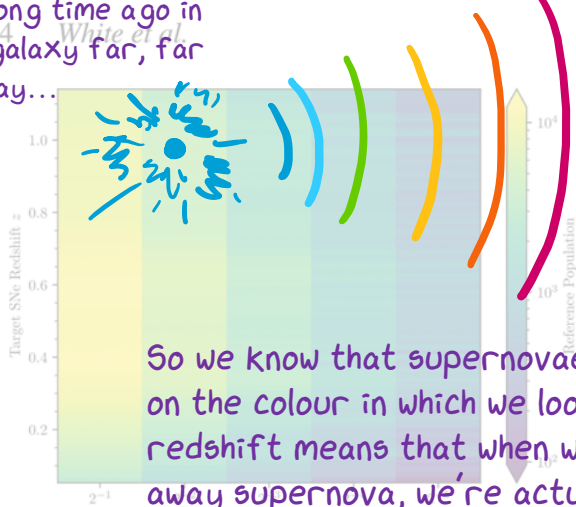


Figure 3. For each of the SNe Ia in our sample, we constructed a reference light curve with a  $\delta = 2$  parameter according to Equation 3, with  $\Delta\lambda_f$  band FWHM. We counted how many data points populated the reference curves (i.e. the number of *points* in Fig. 4 for example) changing  $\delta$  in integer steps of powers of 2. The plot shows the reference population for a target SN measured in the observer frame  $I$  band, and is largely similar for the different bands differing only by a constant multiplicative factor. The plot is an analogous plot in a bluer band would see the colour distribution shifted downwards in target redshift.

If we want to compare supernova light curves across different redshifts, we need to account for these effects.

We proposed using a mathematical selection function\* to carefully choose light curves at certain redshifts and in

certain colours so that we get a sample that should all have

the same shape.

high redshift (whose observations had comparatively low S/N). In the analysis, we did not attempt to fit SNe light curve widths to their light curve evolution over time, and if their reference curve had fewer than 100 data points (discussed in Section 4). This was done on a per-band basis; we estimated the width of each SN light curve in each band where it satisfied these criteria. Individual light curves were also omitted from the analysis if the  $\chi^2$  width fitting did not converge. All together, after these quality cuts we were left with width measurements of 1504 unique SN Ia across the dataset.

## What do \*we\* do in the paper?

### 4 FITTING SUPERNOVA PHOTOMETRY TO A REFERENCE LIGHT CURVE

If time dilation is real, we should see that supernovae take longer at higher redshift (from our perspective). That means that if we stack light curves from various redshifts that should have the same shape, the higher redshift ones will appear wider!

Our method is unique in that we use \*only\* the data from the Dark Energy Survey—no other supernovae were hurt in the making of this paper.

## Space and time

to anyone target SN. The target  $I$  is the SN whose width we are trying to measure.

Because the shape of a SN I light curve is dependent on the rest-frame effective wavelength at which it is observed (Fig. 1; see also Takatori et al. 2008; Benetti et al. 2012), the reference photometry must be composed only of light curves that have the same (or very similar) intrinsic shape as the target SN. Hence, one must choose reference photometry that matches the rest-frame effective wavelength as the target light curve. This effect is shown in Fig. 2, where, for example, we might compare a low- $z$  supernova in some band against the photometry from that band. If we compared with the same or similar) rest frame effective wavelength. We can compare the photometry between two bands provided that their rest-frame effective wavelength (and hence their light curve shape/evolution) is alike.

To find the best reference population for a target light curve in some band against all of the photometry from that band, we would expect a non-linear change in the target's width in a high-vs-low-redshift plot. The explanation for this lies in the fact that SNe I spectra get redder over time; the light curves measured in a redder band are intrinsically wider than those measured in a bluer band as shown in Fig. 1. Hence, with this hypothetical method (comparing to all bands) we would end up with a target with an average rest-frame curve for a high redshift SNe which would bias the obtained width to an intrinsically dimmer value. Conversely, we would be biased towards smaller widths for a target with a few redshift supernovae. To avoid this bias, we use the aforementioned method of only using the reference population with the same rest-frame wavelength as our target light curve.

To find relevant light curves to populate the reference curve, we pick all light curves out of a calculated redshift range. To fit a single (target) SN light curve at redshift  $z$  imaged in a band of central wavelength  $\lambda_f$ , we can populate the reference curve with SNe within the redshift range

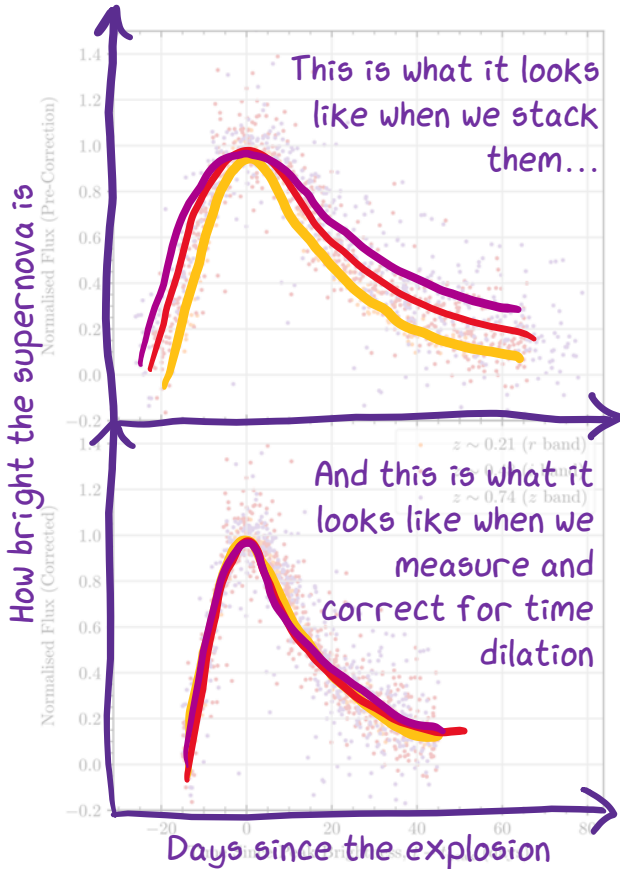
$$\frac{\lambda_r(1+z)}{\lambda_f} - \delta \frac{\Delta\lambda_f}{\lambda_f} \leq 1 + z_r \leq \frac{\lambda_r(1+z)}{\lambda_f} + \delta \frac{\Delta\lambda_f}{\lambda_f} \quad (3)$$

This equation essentially says that if we want to compare with a supernova at a very high redshift, we need to collect light in a redder filter so that we're seeing the same type of stuff!

We show in Fig. 3 the number of points in the reference curves (the reference population) as a function of redshift for all the DES-SN with a variable  $\delta$  parameter. Ideally, this  $\delta$  parameter should be as small as practical to ensure that the reference curve is consistent in shape (i.e. the spread of rest frame effective wavelengths is small). In practice, we find a value of  $\delta = 2$  is the minimal value that provides a large enough reference population for high-/low-redshift SNe (on the order of  $\sim 10^4$  needed to satisfy the Section 3 criteria at  $z > 0.5$ ). As we increase  $\delta$  (and hence the number of curves in the DES-SN sample), we note that the reference population is large (we even have  $\sim 10^4$  points at  $z > 1$ ).

After populating the reference curve with data points, we then normalise the photometry in flux, as the curve is populated with curves from the same SNe and the total light curve must be homogeneous in flux. To do this, we utilised the peak flux in the SALT3 model light curves provided for each SNe. The data in each constituent curve is normalised by this value before being added to the reference. For convenience we also use the time of peak brightness given by SALT3 as the reference point about which to stretch the light

\*For astrophysics, we're kind of light on the math in this paper!



When we take orange light from redshift 0.2 supernovae, red light from redshift 0.5 supernovae, and infrared light from redshift 0.75 supernovae, the light curves should look the same! But the top plot shows that the redder light curves (from higher redshifts!) are \*wider\*. This is time dilation in action!

After the flux of the reference curve is normalised, we see that the different bandpass data in the curve are temporally stretched (see the colour gradient of the top plot in Fig. 4). As the redder bandpasses are sampling longer lags than the bluer ones, this is a measure of time dilation. Without assuming our expected cosmological time dilation of  $(1+z)$ , we can scale the data in *all* of the reference curves by a factor of  $(1+z)^b$  to shift each colour curve in a reference and  $b$  is a free parameter. We posit that minimising the dispersion across the entire sample is a good proxy for the optimal temporal scaling, simultaneously minimising the dispersion in time. Hence, finding the value of  $b$  that minimises the flux scatter gives us a time dilation factor.

To investigate this, we generated reference curves for each of the different colours line up, we've got our time dilation measurement!

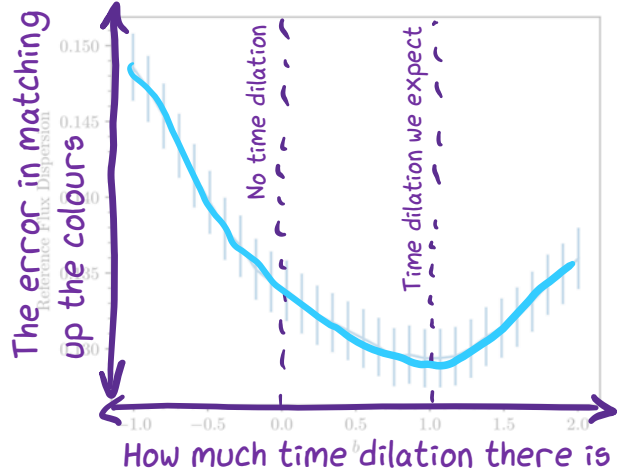


Figure 5. By scaling the reference photometry in time according to  $(1+z)^b$  for some free parameter  $b$ , we find  $b=1$  minimises the reference flux dispersion across the entire sample, i.e., the zero flux dispersion case. This uses the median dispersion of flux across the entire sample of normalised reference light curves in each band (here averaged for the  $riz$  bands), where the errorbars indicate one standard deviation in these values. We note that this figure yields a signal of  $(1+z)$  time dilation in the DES dataset, independent of the rest of the analysis.

target SNe per observing band and scaled the data in time according to the aforementioned relation in terms of  $b$  (Fig. 4) shows the scaling for  $b=1$  (no dilation). We then took the same data into 30 equal-width time bins and found the standard deviation of the fluxes in each bin and added up all the standard deviations as a representative estimate of the total flux scatter for that reference curve with that tested  $b$  value. We then took the median of these values over all the SNe reference curves and our measure of the dispersion for that  $b$ , which is shown in Fig. 5. That is, our reference flux dispersion is given by eqn 4:

$$\sigma_{ij}(b) = \text{median}(\sigma_{ij}(b) | \forall j \in (1, \dots, 30) | \forall i \in (1, \dots, N_{\text{SN}})) \quad (4)$$

We fit a factor of time dilation of  $(1+z)^b$ , where  $z$  is the redshift value and  $b$  is just some number;  $b=0$  means no time dilation and  $b=1$  is the time dilation we expect in our universe.

If there was no time dilation we would expect the minimum dispersion to be at  $b=1$ , but in fact it is at  $b < 1$ , as indicated in Fig. 5. The fact that we find  $b < 1$  is evidence for time dilation of the expected form. This is a rough but completely model-independent measure of time dilation and its value is best stated as

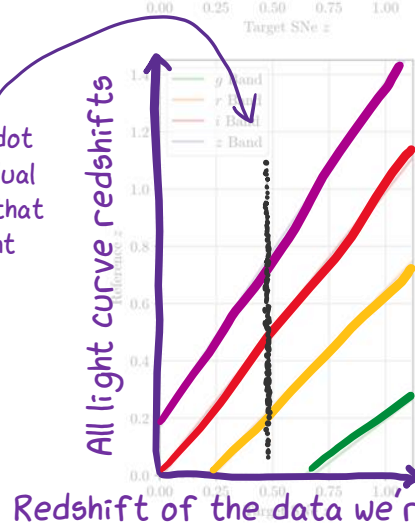
#### 4.3 Second measure of time dilation: Finding each light curve

Cosmology can rest easy! For now...

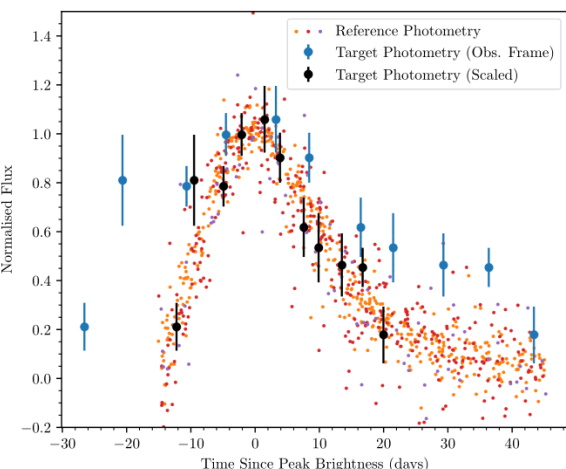
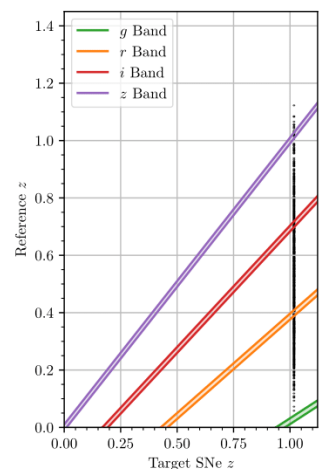
After constructing the reference curves for a target SN, we are ready to fit for the width,  $w$ , of each individual target light curve and look for a trend with redshift. This method enables a more precise measure of  $b$ .

Another way that we can find time dilation is to find the 'width' of each individual supernova light curve.

We can make the 'stacked' light curve (corrected for time dilation using the result from before) and fit an individual light curve to it to find how wide it is.



This is how we choose what light curves go into the stacked light curve – no math needed here. Wherever the black dots intersect the coloured bands, we can take those light curves observed in that colour and put them in the stacked curve! These light curves should all have the same shape.



Here's one of the unedited plots from the paper now that we what's going on!

Figure 6. We show the reference curve construction and subsequent target SN fit for 3 SNe at redshifts  $z = 0.22$ ,  $z = 0.43$ , and  $z \approx 1.02$  and in fitting bands  $r$ ,  $i$ , and  $z$  respectively (in descending order). The left plots show the allowed ranges for reference curve SN sampling given the target redshift (and  $\delta = 2^{-4}$ ). The vertical line of dots is plotted at the target SN redshift, with each dot representing the redshift of a DES supernova (vertical axis). The dots that fall in the narrow coloured bands are the SNe that make up the reference population, as those data all share approximately the same rest-frame wavelength in their respective bands. The right plots show the constructed  $(1+z)$  time-scaled reference curve (small coloured points) with respect to the target SN photometry (blue points) and subsequent target photometry scaled on the time axis to fit the reference (best-fit widths of 1.42, 1.49, and 2.17 respectively). Due to the statistics associated with such large reference curve populations, the contribution of any individual reference point uncertainty to the overall reference curve uncertainty is negligible and not plotted; the uncertainty in the target data has a much higher contribution to the uncertainty in the fitting.

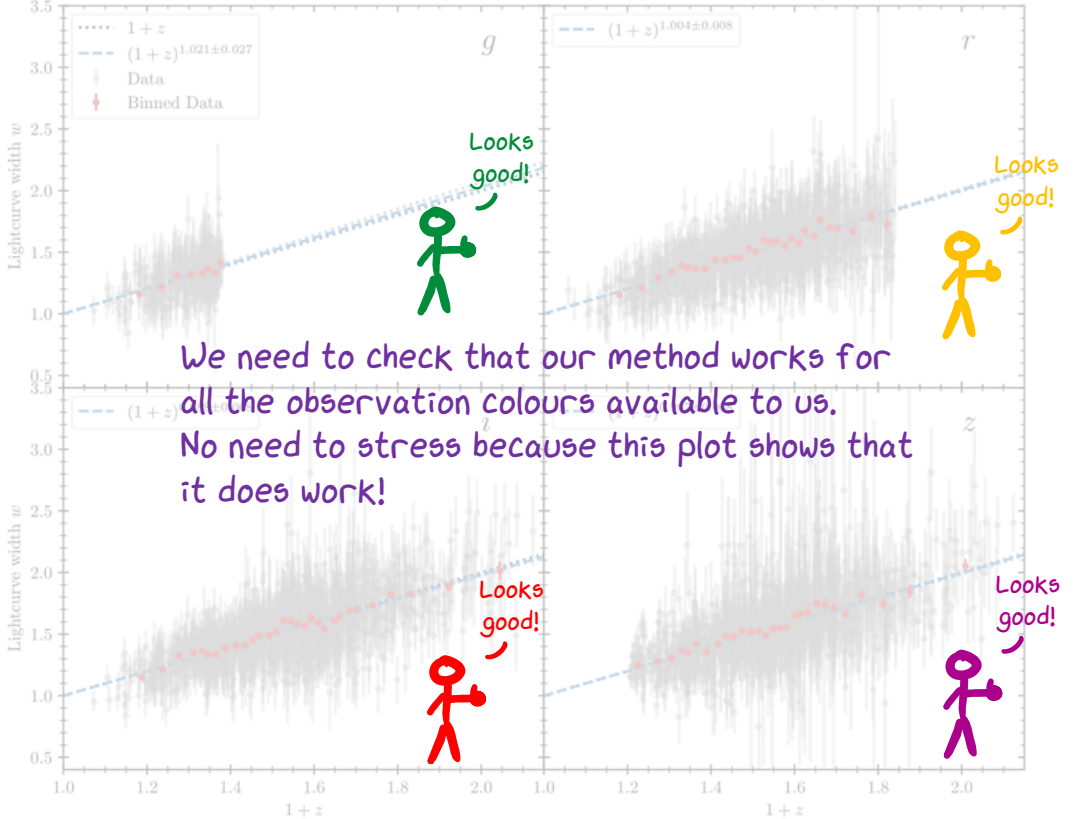


**Figure 7.** Using the reference-scaling method described in Section 4.3, we plot the fitted SNe widths of light curves observed in the  $g$ ,  $r$ ,  $i$ , and  $z$  bands (left to right, top down respectively). The lines of best fit (blue dashed) are in excellent agreement with the expected  $(1+z)$  time dilation (black dotted). The binned data are purely to visualise rough trends in 50 data point bins. 361 SNe in the  $g$  band passed the quality cuts described in Section 3, while the  $r$  band has 1380 SNe, the  $i$  band 1465, and the  $z$  band 1381. The reduced chi-square values,  $\chi^2_{\nu}$ , of each fit (left to right, top down) are 0.537, 0.729, 0.788 and 0.896 respectively.

We first normalise the target data to the peak flux using the SALT3 fit (as with the reference curves). The free parameter in the fit is the scaling parameter  $1/w$ , whereby changing this value would stretch and squash the data relative to  $t_{\text{peak}}$ .

This is us describing the math and code that we used to find the widths of the light curves. We don't use a particularly difficult or advanced method, but it's accurate for our purposes and runs quickly on a personal computer.

$$F_i(t) \simeq f_i \left( \frac{t - t_{\text{peak}}}{w} \right)$$

and change  $w$  until the data most closely matches the reference. Here,  $f_i(t)$  corresponds to the  $i$ th target light curve;  $F_i(t)$  corresponds to the  $i$ th reference curve where each point is now scaled in time by  $(1+z)$  relative to  $t_{\text{peak}}$  as per the results of Section 4.2.

To fit the target light curve width using its reference curve, we minimised the  $\chi^2$  value of the differences in the target flux compared to the median reference flux in a narrow bin around time values of the target photometry. That is, for each target light curve we minimised

$$\chi^2_i = \sum_j^{N_p} \frac{(f_{ij} - \text{Med}\{F_i(t) \mid \forall t \in [t_{ij}/w - \tau, t_{ij}/w + \tau]\})^2}{\sigma_{ij}^2} \quad (6)$$

for  $N_p$  number of points in the  $i$ th target SN light curve ( $f_i$ ). The points in the reference curve ( $F_i$ ) bin that are averaged and compared

to each target SN flux value ( $f_{ij}$  – with error  $\sigma_{ij}$ ) are selected within the time range  $[t_{ij}/w - \tau, t_{ij}/w + \tau]$ ; here  $t_{ij}$  is the time since peak brightness of each target data point scaled by the fitted width  $w$ , and  $\tau$  is the width of the narrow bin around the central time value  $t_{ij}$ .

During the fitting process, the bounds of this narrow bin around each time value changes as the target data is scaled in time but remains centered on  $t_{ij}$ . We choose  $\tau = 1/2\tau_0$  of 4 rest-frame days (i.e.  $\pm\tau = \pm 2$  of a central value); ideally this would be as low as practical to minimise noise in the fit. We use the target data point position and the reference curve slice, but needs to be large enough to provide a sufficiently populated sample of the reference to compare to. We find that a width of 4 days (just the width of a minor tick span in Fig. 4) is low enough that the reference curve does not significantly change in flux but still contains enough points even for high/low redshift target SNe with small reference populations. With this  $\tau = 2$  value we find  $\gtrsim 50$  data points per time slice at the highest and lowest redshifts, where a  $\tau = 1$  yields a prohibitively small  $\lesssim 20$  data points per slice even in the most well sampled photometric band ( $i$ -band).

In fitting the data, we did not include any target SN data points that extended past the maximum time value in the reference curve; the late-time light curves of SNe dwindle slowly and are less constraining for width-measurements than those near the peak. We also omitted any points that had observation times prior to the first reference curve point from the fitting procedure.

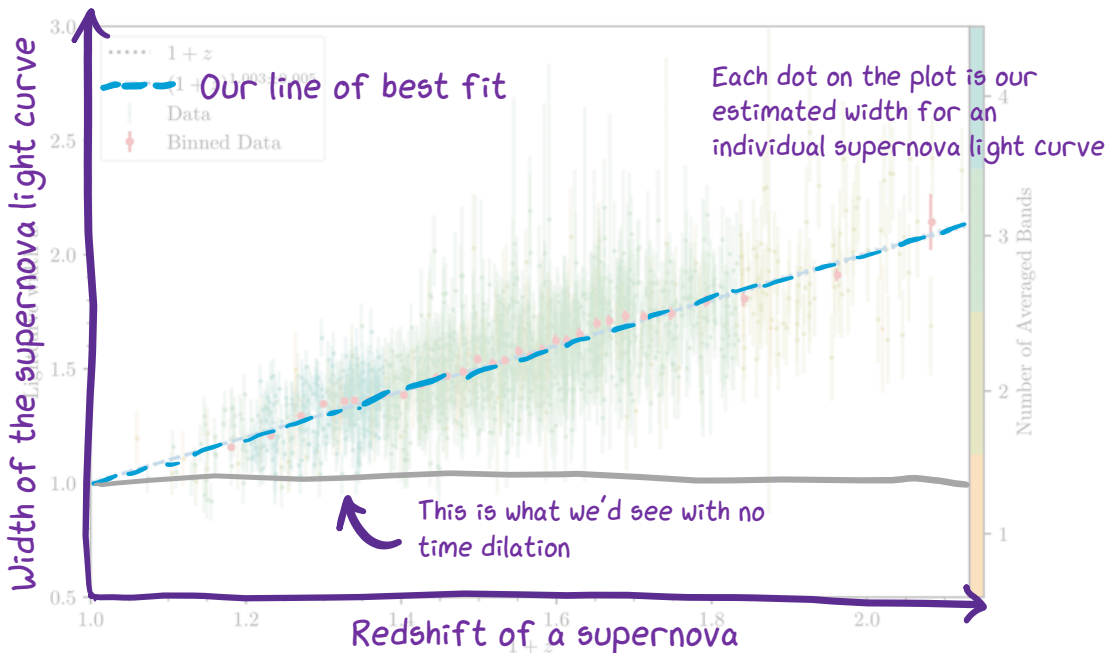


**Figure 8.** We show here the width value for each SNe averaged across all available bands. Since cosmological time dilation is independent of the observed band of any SN, we can fit the widths in all bands together to get the time dilation. The fit is  $w = (1 + z)^{1.003 \pm 0.005}$ . Time dilation (reduced chi-square  $\chi^2_{\nu} = 1.441$ ) is comprised of the 1504 unique SNe across the 4 bandpasses, where the error bars here are the Gaussian propagation of errors in the final model. This is significantly better than the power law fit in Fig. 4, which has a linear model fit to the data recovers  $w = (0.988 \pm 0.016)(1 + z) + (0.020 \pm 0.024)$  (with the same  $\chi^2_{\nu}$  to 4 significant figures), consistent with our power model fit above.

We note that this method of fitting is not fundamentally limited by target SN data with pre-peak high-precision observations in each band. Given enough target data (on the order of several well spaced points in time), the matching of data to the corresponding reference curve phases is unique regardless of whether pre-peak data is available.

In science we usually can never claim a perfectly precise result and need to discuss our uncertainty in our model fits; this is where that 'plus or minus' 0.015, or  $\pm 0.015$ , came from in our result. This means that we would normally expect the true result to be somewhere in that range of our found result.

An example of how a reference curve is created is shown in Fig. 4. We note that while the width fitting for the whole dataset was calculated in all four DECam bands, only the  $i$  band data encompasses the entire redshift range of the DES-SN sample. Due to the sparser, less frequent high-redshift data, the  $g$  and  $r$  filters are unable to detect SNe at sufficiently high redshift ( $\geq 0.4$  and  $\geq 0.85$  respectively) as the observed wavelengths shift to lower emitted wavelengths (see Fig. 2 of DES Collaboration et al. 2024) and become fainter as a re-

sult. Fig. 8 shows that fitting  $w = (1 + z)^b$  in the  $z$ -band would require relatively redshifted SNe in the other bands to compute the reference; hence there is an inherent redshift floor for  $z$ -band fits leaving the  $i$ -band as the only suitable bandpass for the entire redshift range.

The widths obtained in all four bands separately are shown in Fig. 7. We see the truncated  $g$ ,  $r$  and  $z$  band data, and fit widths that are significantly different from each other. The  $i$ -band data is the most complete and has the lowest uncertainty. The averaged widths of all the bands are shown in Fig. 8, again showing the significant difference between the four bands.

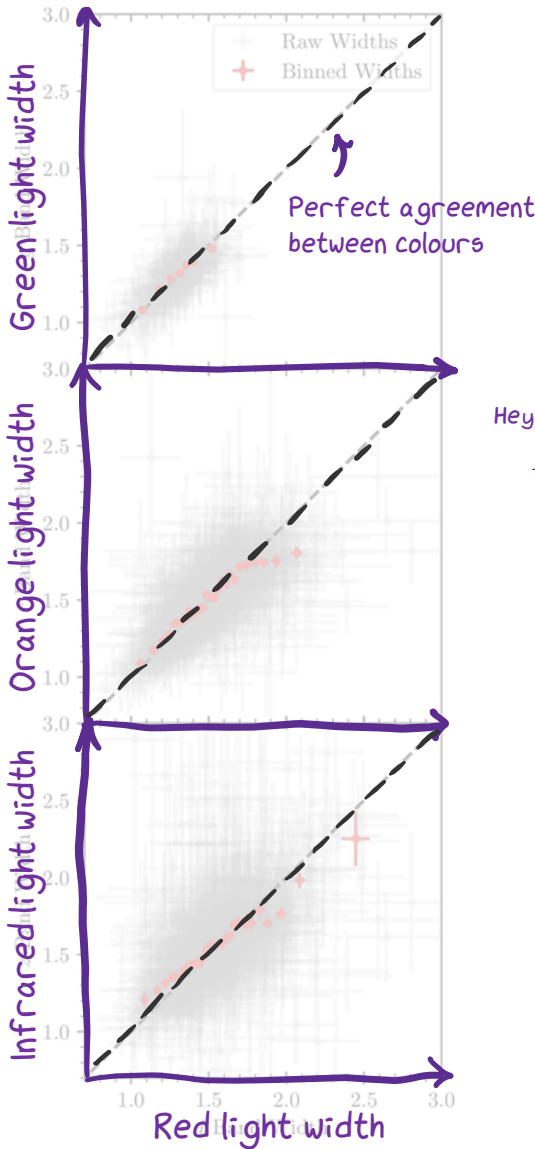
As mentioned in the introduction, this method has an element of circularity because we de-time-dilated the observed light curves to create a reference curve. However, this is not a problem because we are not just getting the answer we put in we repeated the analysis with different time dilation values and got different reference light curves more noisy and wider (like the top plot of Fig. 4). If the dilation is itself we should get a consistent  $w = 1.0$  fit in this case. However, if  $(1 + z)^b$  time dilation is what we should find, the slope inconsistent with  $b = 0$  and an intercept offset from  $w = 1.0$  is what we expect. Spoiler: it's only possible to get a real signal when we correct for it in our stacked light curve!

## Now let's talk about what we found

As we see in Fig. 7, there is a clear and significant non-zero time dilation signature in the DES SN Ia dataset, conclusively ruling out any static universal models. Our method described in Section 4 detects a time dilation signature in all of the  $g$ ,  $r$ ,  $i$ , and  $z$  DECam bandpasses we find, as expected, that the  $b = 0$  result is excluded strongly by this test (see Appendix and Fig. C4).

We note that while the width fitting for the whole dataset was calculated in all four DECam bands, only the  $i$  band data encompasses the entire redshift range of the DES-SN sample. Due to the sparser, less frequent high-redshift data, the  $g$  and  $r$  filters are unable to detect SNe at sufficiently high redshift ( $\geq 0.4$  and  $\geq 0.85$  respectively) as the observed wavelengths shift to lower emitted wavelengths (see Fig. 2 of DES Collaboration et al. 2024) and become fainter as a result. Probably not over here. INI-22-000, (2024)

Is the true value here?  
Or here?



We need to check to make sure that we're finding roughly the same width in each band for each SNe should be intrinsically correlated as they arise from the same event. We can do this by looking at the agreement between bands. We plot their agreement relative to the  $i$  band in all of the different colours we look at each supernova in. On average, we do!

as expected. The power-law fits to the data in each bandpass are all consistent with the expected  $(1 + z)$  law to within  $2\sigma$ .

Since there is a well documented stretch-luminosity relationship in Ia light curves (Phillips 1993; Phillips et al. 1999; Kasen & Woosley 2007), it is possible that Malmquist bias could skew the data to larger widths at high redshift where we may not see the less-luminous SNe. Regardless, this does not greatly influence the quality of our fits since the DES SN data extend to such high redshifts that the

You might expect that we see preferentially brighter objects when looking very far away—imagine your friend shining a flashlight at you as they walk away. Eventually, when they make good distance, you won't be able to see them anymore unless they get a brighter flashlight! Near Far

Hey, ow! As a test of the robustness of our method, we reran all the width-fitting steps with a requirement of pre-peak observations in each light curve. ~~and most~~ this changed the power law fit by  $\Delta b = -0.004$  for the  $g$  band. The calculated  $b$  values in the other bands were increased by one or two thousandths (including the averaged fit of Fig. 8), or not at all. Interestingly, including this pre-peak restriction reduced our ~~Do not go gentle~~ SNe widths by only 24 in total. This reduction does not necessarily say if this method is robust at fitting light curves without pre-peak data, and future analyses may look at purposefully degrading the dataset (e.g. by manually removing pre-peak data) investigating this.

**Interestingly, the Dark Energy Survey Type Ia supernova sample avoids this bias quite a lot! Even if this bias were present in our data, it would only contribute  $<15\%$  to the light curve widths which is very small compared to the  $>100\%$  effect of time dilation at high redshift. At**

To avoid de-redshifting reference light curves we devised another method. In this approach, we take a set of data points and fit a posterior distribution of  $b$ . This entailed generating a reference curve without first scaling it in time (as in the second method), and fitting time dilation signal.

We also looked at another, more advanced method that would mean that we \*wouldn't\* need to correct for time dilation in the stacked light curve before fitting for light curve widths. We found that this wasn't practical as we'd need even more data than we have: remember that DES has given us the largest sample of data at this high a distance, so we'd need a truly huge dataset to do this.

(which will be the topic of future work). We instead performed the analysis with flux-scatter minimisation and width-fitting methods as these have been previously found to give similar constraints. In addition to a unified (in phase) reference curve composed of all available bands, we similarly note that our method with the DES dataset would disallow the null hypothesis of no cosmological time dilation to a 0.3% level (200 times more precise than what was previously possible). The evolution of the stretch of supernova light curves as a function of redshift was found to be small, with a likely upper bound of  $\sigma_b^{\text{sys}} \simeq 0.01$ . Given the current limit on the variance of  $\sigma_b^{\text{sys}} + \sigma_b^{\text{stat}} \simeq 0.015$  this remains the most precise constraint on cosmological time dilation.

## The take home message:

### CONCLUSIONS

Using two distinct methods, we have conclusively identified  $(1+z)$  and  $\Omega_m$  using the light-curve shape and photometry of 1504 SNe Ia from the Dark Energy Survey that met our quality cuts. We made this detection with the most model-independent method yet in the literature, without the need for Hubble-like superluminae. For both methods, we create a ‘reference curve’ unique to each supernova type (andpass) which describes the expected light curve shape without accounting for the stretch variation associated with SNe Ia subtypes. Doing this reduces the number of free variables (the number of CNO shell frequency of imitating and the redshift range) and would not be possible with a significantly smaller sample. This effectively certifies that the standard烛光模型 (SN Ia should be standard candles/clocks).

Using this reference curve we show an inherent preference of  $\sim 1\%$  time dilation in the data, first by minimising the flux scatter in the data via a redshift-dependent temporal scaling, and then with a width-fitting technique. The latter approach allows for numerical estimates with uncertainty with which we obtain a factor of  $\sim 1.1 \pm 0.05$  in the standard烛光模型. This provides a constraint on cosmological time dilation yet

We discuss factors and choices that affect our fits and notably see no indication that Malmquist bias or light-curve stretch significantly impacts our results. Our results infer a cosmological time dilation that is qualitatively (though not quantitatively) consistent with previous findings (Gibb & Scolnic 1996; Goldhaber et al. 2001; Blomqvist et al. 2001; Riess & Brout 2023), with more SNe Ia and at a higher redshift than before.

### ACKNOWLEDGEMENTS

RMTW, TMD, RCa, SH, acknowledge the support of an Australian Research Council Australian Laureate Fellowship (FL180100168) funded by the Australian Government. AM is supported by the ARC Discovery Early Career Researcher Award (DECRA) project number DE23010005.

Funding for the DES Projects has been provided by the U.S. Department of Energy, the U.S. National Science Foundation, the Ministry of Science and Education of Spain, the Science and Technology Facilities Council of the United Kingdom, the Higher Education Funding Council for England, the National Center for Supercomputing Applications at the University of Illinois at Urbana-Champaign, the Kavli Institute of Cosmological Physics at the University of Chicago, the Center for Cosmology and Astro-Particle Physics at

the Ohio State University, the Mitchell Institute for Fundamental Physics and Astronomy, and the Romanian Ministry of Education and Research, FAPESP, Fundação Carlos Chagas Filho de Amparo à Pesquisa do Estado do Rio de Janeiro, Conselho Nacional de Desenvolvimento Científico e Tecnológico and the Ministério da Ciência, Tecnologia e Inovação, the Deutsche Forschungsgemeinschaft and the Helmholtz-Gemeinschaft.

**It takes a \*lot\* of funding for a lot of people to allow us to do these kind of studies. Even though the light from these supernovae is raining down everywhere on Earth, it takes a huge telescope to collect it all reliably.**

The Collaborating Institutions are Argonne National Laboratory, the University of California Berkeley, the University of Cambridge, Centro de Investigaciones Energéticas, Medioambientales y Tecnológicas-Madrid, the University of Chicago, University College London, the DES-Brazil Consortium, the University of Edinburgh, the Eidgenössische Technische Hochschule (ETH) Zürich, Fermi National Accelerator Laboratory, the University of Illinois at Urbana-Champaign, the Institut de Ciències del Espai (IEEC/CSIC), the Institut de Física d'Altes Energies, Lawrence Berkeley National Laboratory, the Ludwig-Maximilians Universität München and the associated Excellence Cluster Universe, the University of Michigan, NSF's NOIRLab, the University of Nottingham, The Ohio State University, the University of Pennsylvania, the University of Portsmouth, SLAC National Accelerator Laboratory, Stanford University, the University of Sussex, Texas A&M University, and the OzDES Membership Consortium.

Based in part on observations at the Cerro Tololo Inter-American Observatory (CTIO) and NOIRLab (NOIRLab Prop ID 2012B-0001; PI: J. Frieman), which is managed by the Association of Universities for Research in Astronomy (AURA) under a cooperative agreement with the National Science Foundation.

The DES data management system is supported by the National Science Foundation under Grant Numbers AST-1138766 and AST-1536171. The DES participants from Spanish institutions are partially supported by MICINN under grants ESP2017-89838, PGC2018-094773, PGC2018-102021, SEV-2016-0588, SEV-2016-0597, and SEJ-2019-09140. This research has received funding from the European Union. IFAE is partially funded by the CERCA program of the Generalitat de Catalunya. Calculations in these results has received funding from the European Research Council under the European Union's Seventh Framework Program (FP7/2007-2013) including ERC grant agreements 240672, 291329, and 306478. We acknowledge support from the Brazilian Instituto Nacional de Ciéncia e Tecnologia (INCT) do Universo (CNPq grant 46476/2014-2).

This manuscript has been authored by Los Alamos National Laboratory, LLC under Contract No. DE-AC02-06CH11355 with the U.S. Department of Energy, Office of Science, Office of High Energy Physics.

## Want to try it yourself?

### DATASETS

The data are available on Zenodo and GitHub as described in the All of the data is now publicly available and DES-SN5YR data release paper (Sanchez et al. 2024). The generated code and source code used to generate these plots are included in the public GitHub (see Code Availability section), as are supplementary plots not included in the paper.

Dealing with this much data is only possible with programming! The code we wrote uses popular and well tested packages

The code we wrote is also publicly available, so you can take a look at my spaghetti code if you'd like! There's also some bonus plots on our GitHub repository that we didn't include in the paper.

## Whose work did we build on?

- Scott T. M., et al., 2018, *ApJ*, 855, 18  
 Blondin S., et al., 2008, *ApJ*, 682, 724  
 Bellini S., et al., 2019, *A&A*, 626  
 Branch D., Wheeler J., et al., 2017, Observational Properties, Springer Berlin Heidelberg, Berlin, Heidelberg, pp. 107–133-662-55054-0\_20, doi:10.1007/978-3-662-55054-0\_20  
 Every new piece of science builds on the shoulders of giants. We're continuously improving, refining, finding new results based on the work that other smart people have published. For this paper we had to read a bunch of other papers to learn more about what's been done in the past, intricacies about supernovae, and the Dark Energy Survey data!  
 Foley J., et al., 2015, *AJ*, 150, 150  
 Foley R. A., Filippenko A. V., Leonard D. C., Klessel P., Nugent P., Perlmutter S., et al., 2022, *J. Astron. Soc. Australia*, 39, e046  
 Goldhaber G., et al., 1997, Observation of Cosmological Time Dilation Using Type Ia Supernovae, *Science*, 275, pp. 777–784, doi:10.1126/science.275.5305.777  
 Guy J., et al., 2007, *A&A*, 466, 11  
 Harris C. R., et al., 2020, *Nature*, 585, 357  
 Howell D. A., Sullivan M., Conley A., Carlberg R., 2007, *ApJ*, 667, L37  
 Hoyle F., Fowler W. A., 1960, *ApJ*, 132, 565  
 Hunter J. D., 2007, Computing in Science & Engineering, 9, 90  
 Kasen D., Woosley S. E., 2007, *ApJ*, 656, 661  
 Kenworthy W. D., et al., 2021, *ApJ*, 923, 265  
 Kessler R., et al., 2015, *AJ*, 150, 172  
 Leibundgut B., Sullivan M., 2018, *Space Sci. Rev.*, 214, 57  
 Leibundgut B., et al., 1996, *ApJ*, 466, L21  
 Lewis G. F., Brewer B. J., 2023, *Nature Astronomy*, 7, 1598  
 Matheson T., et al., 2008, *AJ*, 135, 1598  
 Möller A., de Boissière T., 2020, *MNRAS*, 491, 4277  
 Möller A., et al., 2022, *MNRAS*, 514, 5159  
 Möller A., et al., 2024, *arXiv e-prints*, p. arXiv:2402.18690  
 Müller-Bravo T. E., et al., 2022, *A&A*, 665, A123  
 Nelder J. A., Mead R., 1965, *The Computer Journal*, 7, 308  
 Nicolas N., et al., 2021, *A&A*, 649, A74  
 Norris J. P., Nemiroff R. J., Scargle J. D., Kouveliotou C., Fishman G. J., Meegan C. A., Paciesas W. S., Bonnell J. T., 1994, *ApJ*, 424, 540  
 Phillips M. M., 1993, *ApJ*, 413, L105  
 Phillips M. M., Lira P., Sunzelt N. B., Schommer R. A., Hamuy M., Maza I., 1991, *ApJ*, 375, 63  
 It's great to live in a time when so many are given the opportunity to study the Universe and share what they find.  
 Piran T., 1992, *ApJ*, 389, L45  
 Riess A. G., et al., 2019, *Reaching for the Last Decade of the Cosmological Constant*, 15, 15  
 Rust J. W., 1997, PhD thesis, Oak Ridge National Laboratory, Tennessee  
 Sanchez et al., 2024, in prep  
 Seconi G., et al., 2023, *ApJ*, 954, L31  
 Smith M., et al., 2020, *AJ*, 160, 267  
 Takanashi N., Doi M., Yasuda N., 2008, *MNRAS*, 389, 1577  
 Tripp R., 1998, *A&A*, 331, 815  
 Vincenzi M., et al., 2024, *arXiv e-prints*, p. arXiv:2401.02945  
 Virtanen P., et al., 2020, *Nature Methods*, 17, 261  
 Wang L., Goldhaber G., Aldering G., Perlmutter S., 2003, *ApJ*, 590, 944  
 Wilson O. C., 1939, *ApJ*, 90, 634

Zwicky F., 1929, *Proceedings of the National Academy of Sciences*, 15, 773  
 pandas development team T., 2023, pandas-dev/pandas: Pandas, doi:10.5281/zenodo.8364959, <https://doi.org/10.5281/zenodo.8364959>

## Now for some bonus content!

### APPENDIX A: STRETCH DRIFT WITH REDSHIFT

There is evidence that the stretch distribution of SNe evolves with redshift, as the fraction of older and younger progenitors evolves. Nicolas et al. (2021) give the following relation for the evolution of the SN stretch distribution,

While we were writing the paper we came across an interesting study that suggests that supernova light curves really are somewhat \*intrinsically\* wider at high redshift. We don't yet know why this is, but as with any good science we can model it!

$$\delta(z) = \delta(\bar{z})N(\mu_1, \sigma_1^2) + (1 - \delta(\bar{z}))\left( (N(\mu_2, \sigma_2^2)) - \bar{a} \right)N(\mu_2, \sigma_2^2), \quad (\text{A1})$$

where  $N(\mu, \sigma^2)$  is a normal distribution with mean  $\mu$  and variance  $\sigma^2$ . The values of the parameters are  $\bar{z} = (0.51, 0.37, 1.22, 0.64, 156, 0.87)$ , and the fraction of young supernovae in the population is given by,

$$\delta(\bar{z}) = \left( \frac{K^{-1}(1 + z)^{-2.8}}{1 + z} \right)^{-1} \quad (\text{A2})$$

The distribution given by equation (A1) is shown in the upper panel of Fig. A1 for several redshifts, where the vertical dashed lines show the resulting change in the mean  $x_1$ . The relationship between  $x_1$  and the stretch of the supernova is given by (Guy et al. 2007),

$$s = 0.08 + 0.091z + 0.003z^2 - 0.00075z^3 \quad (\text{A3})$$

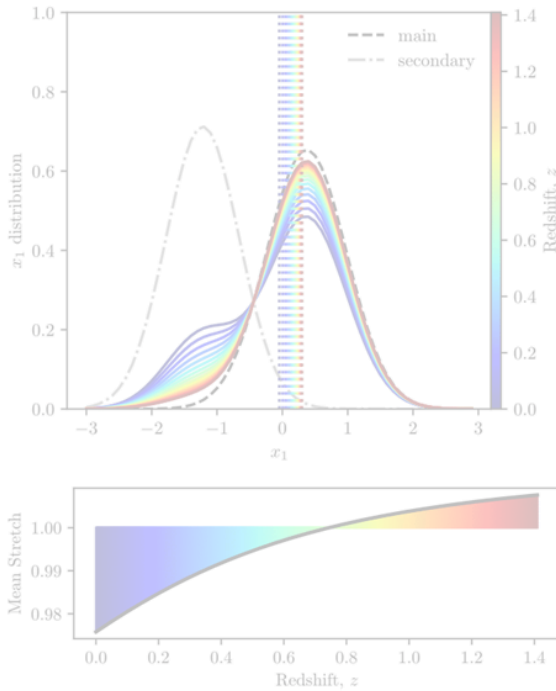
and this is shown in the lower panel of Fig. A1.

Since light curve width is directly proportional to stretch, that means the light curves at higher redshift are approximately 3% wider than those at  $z = 0$ . This is therefore substantially subdominant to the 10% width variation due to time dilation over the same range.

Crunching the numbers shows that this 'redshift drift' in the width of light curves would only change our signal by ~3% if we did see it!

Despite this consistency of fit in the DES sample, it is hard to quantitatively determine if the lightcurve widths could be fit if equation (A1) holds. Thankfully this over-estimation can be reduced if there is a non-linear evolution of the intrinsic widening included, you would actually get a line of  $\Delta t \approx 1.03(z + C) - 0.02(z + C)^2$  (Fig. A2). Note while this would change the slope by ~3%, this is in contrast to the recovered linear model fit in the Fig. 8 caption, hence indicating that this redshift-dependent stretch is not evident in the DES-SN5YR data.

The impact of high-redshift supernovae tending to have a few percent wider stretch than their low-redshift counterparts would cause us to slightly overestimate  $b$ . The magnitude of the impact on  $b$  depends on your redshift distribution, we estimate a shift of  $|\Delta b| \lesssim 0.01$  for the DES data, and we consider this a likely upper limit to the systematic uncertainty on our result. Since our aim in this paper is to fit the light curves with the minimal modelling assumptions (and since we do not see an  $x_1$  trend in our light curve fits) we have chosen not to correct for this trend. Instead we note that any potential effect would only be a small deviation around the slope of  $w/(1+z) \sim 1$  that we see.



**These plots show what we'd expect to happen to our data with the redshift drift, and back up our claim that we don't really see it with the DES dataset.**

**Figure A1.** Upper panel: Distribution of  $x_1$  values predicted by Nicolas et al. (2021). The lower panel (left) shows the evolution of the components of the supernova population. The coloured lines show the total distribution for several different sub-populations, while the grey line shows the evolution of the redshift distribution (in the same colours as the legend). One can see that the mean drifts of the components are very small, indicated by the grey line. The black line shows the evolution of the mean stretch ( $s$ ) of the supernova population with redshift (in the same colours as the legend), indicated by the grey line. The intrinsic light curve width is proportional to  $s$ , and therefore light curves are expected to be about 5% wider at  $z=1$  than at  $z=0$ . This is much less than the factor of two widening due to time dilation.

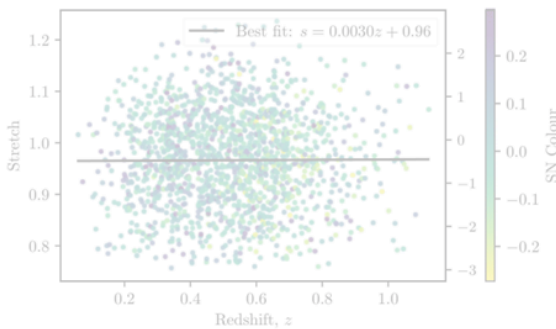
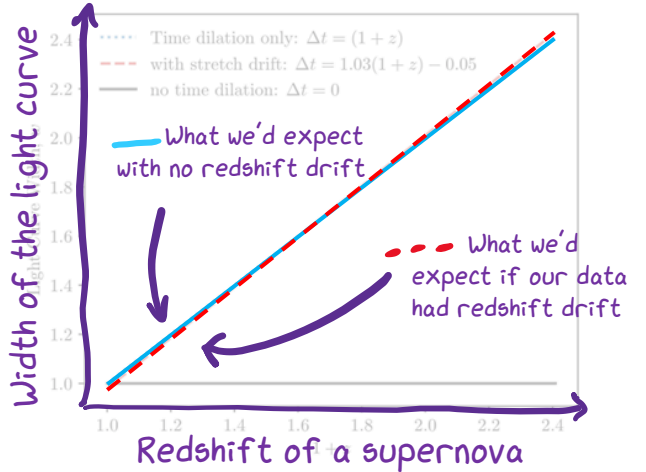


**Figure A2.** The distribution of stretch in the DES-SN5YR data as a function of redshift (calculated from the SALT3 fitted  $x_1$  values using equation A2), with  $x_1$  shown on the right axis. Fitting a straight line to this distribution shows no significant trend in the stretch with redshift.



**Clearly a very small effect!**

**Figure A3.** The effect of adding the predicted stretch evolution of SNe Ia vs redshift to the time dilation. Adding redshift drifts to slightly taper. If this result is present we therefore expect to slightly overestimate  $b$ , as we will attribute that widening to time dilation.

## Bonus content 2: electric boogaloo

### APPENDIX B: REFERENCE CURVE SELECTION DERIVATION

We begin with the definition of redshift,

$$1+z = \frac{\lambda_o}{\lambda_e} \quad (B1)$$

I was a little bit silly and repeatedly messed up this math in the early stages of the project. I wrote it out here so that everyone could see my attempt and correct me if I got it wrong!

$$\frac{\lambda_f}{\lambda_r} \frac{\lambda_e}{\lambda_r} = \frac{\lambda_f}{\lambda_r} \quad (B2)$$

Then, we can rearrange to find an expression for our target redshift  $z_r$  good to remind ourselves that we're not infallible and talking to others helps us improve our work! (B4)

We can then append a term  $\pm \Delta z$  on equation (B4) to give us a range of applicable redshift values as in Section 4.1. Finally, it is useful in the broader context of the paper (and Fig. 3) to show this redshift range in terms of some fraction of the band FWHM of the band that the target SN was observed in,  $\delta \Delta \lambda_f$ . To do this we set  $\Delta z = \delta \Delta \lambda_f / \lambda_f$  and shift the term into the fraction within equation (B4),

$$z_r = \frac{\lambda_r(1+z) \pm \delta \Delta \lambda_f}{\lambda_f} - 1 \quad (B5)$$

which yields the redshift sampling range of equation (3) that we use in the analysis.

## Bonus content 3: it's the last from me!

### APPENDIX C: NULL TEST — NO DE-REDSHIFTING OF REFERENCE LIGHT CURVES

To confirm that our method is able to rule out no time dilation we This is where we describe how badly things mess up when we don't correct for time dilation in the stacked light curves. See the next page to see it in action (it might help to compare with the analogous plot a few pages back).

### AFFILIATIONS

<sup>1</sup> School of Mathematics and Physics, The University of Queensland, QLD 4072, Australia

<sup>2</sup> Sydney Institute for Astronomy, School of Physics, A28, The University of Sydney, NSW 2006, Australia

<sup>3</sup> Centre for Gravitational Astrophysics, College of Science, The Australian National University, ACT 2601, Australia

<sup>4</sup> The Research School of Astronomy and Astrophysics, Australian National University, ACT 2601, Australia

<sup>5</sup> Department of Physics & Astronomy, University College London, Gower Street, London, WC1E 6BT, UK

<sup>6</sup> Cerro Tololo Inter-American Observatory, NSF's National Optical Infrared Astronomy Research Laboratory, Casilla 603, La Serena, Chile

<sup>7</sup> Laboratório Interinstitucional de e-Astronomia - INEx, Rua Gal. José Cristino 77, Rio de Janeiro, RJ - 20921-400, Brazil

<sup>8</sup> Fermi National Accelerator Laboratory, P. O. Box 500, Batavia, IL 60510, USA

<sup>9</sup> Department of Physics, University of Michigan, Ann Arbor, MI 48109, USA

<sup>10</sup> Departamento de Física Teórica and Instituto de Física de Partículas y del Cosmos (IFACOS-UCM), Universidad Complutense de Madrid, 28040 Madrid, Spain

<sup>11</sup> Institute of Cosmology and Gravitation, University of Portsmouth, Portsmouth, PO1 3FA, UK

<sup>12</sup> University Observatory, Faculty of Physics, Ludwig-Maximilians-Universität, Scheinerstr. 1, 81679 Munich, Germany

<sup>13</sup> Center for Astrophysics | Harvard & Smithsonian, 60 Garden Street, Cambridge, MA 02138, USA

<sup>14</sup> Department of Astronomy and Astrophysics, University of Chicago, Chicago, IL 60637, USA

<sup>15</sup> Kavli Institute for Particle Astrophysics & Cosmology, P. O. Box 2450, Stanford University, Stanford, CA 94305, USA

<sup>16</sup> SLAC National Accelerator Laboratory, Menlo Park, CA 94025, USA

<sup>17</sup> Instituto de Astrofísica de Canarias, E-38205 La Laguna, Tenerife, Spain

<sup>18</sup> INAF-Osservatorio Astronomico di Trieste, via G. B. Tiepolo 11, I-34143 Trieste, Italy

<sup>19</sup> Institut de Física d'Altes Energies (IFAE) The Barcelona Institute of Science and Technology, Campus Bellaterra, 08193 Bellaterra (Barcelona) Spain

<sup>20</sup> Hamburger Sternwarte, Universität Hamburg, Goerlitzbergweg 112, 21021 Hamburg, Germany

<sup>21</sup> Centro de Investigaciones Energéticas, Medioambientales y Tecnológicas (CIEMAT), Madrid, Spain

<sup>22</sup> Department of Physics, IIT Hyderabad, Kandi, Telangana 502285, India

<sup>23</sup> Jet Propulsion Laboratory, California Institute of Technology, 4800 Oak Grove Dr., Pasadena, CA 91109, USA

<sup>24</sup> Institute of Theoretical Astrophysics, University of Oslo, P.O. Box 1029 Blindern, NO-0315 Oslo, Norway

<sup>25</sup> Kavli Institute for Cosmological Physics, University of Chicago, Chicago, IL 60637, USA

<sup>26</sup> Instituto de Física Teórica UAM/CSIC, Universidad Autónoma de Madrid, 28049 Madrid, Spain

<sup>27</sup> Institut d'Estudis Espacials de Catalunya (IEEC), 08034 Barcelona, Spain

<sup>28</sup> Institute of Space Sciences (ICE, CSIC), Campus UAB, Carrer de Can Magrans, s/n, 08193 Barcelona, Spain

<sup>29</sup> Centre for Astrophysics & Supercomputing, Swinburne University of Technology, Victoria 3122, Australia

<sup>30</sup> Center for Astrophysical Surveys, National Center for Supercomputing Applications, 1205 West Clark St., Urbana, IL 61801, USA

<sup>31</sup> Department of Astronomy, University of Illinois at Urbana-Champaign, 1002 W. Green Street, Urbana, IL 61801, USA

<sup>32</sup> Santa Cruz Institute for Particle Physics, Santa Cruz, CA 95064, USA

<sup>33</sup> Center for Cosmology and Astro-Particle Physics, The Ohio State University, Columbus, OH 43210, USA

<sup>34</sup> Department of Physics, The Ohio State University, Columbus, OH 43210, USA

<sup>35</sup> Australian Astronomical Optics, Macquarie University, North Ryde, NSW 2113, Australia

<sup>36</sup> Lowell Observatory, 1400 Mars Hill Rd, Flagstaff, AZ 86001, USA

<sup>37</sup> Department of Physics and Astronomy, University of Pennsylvania, Philadelphia, PA 19104, USA

<sup>38</sup> Departamento de Física Matemática, Instituto de Física, Universidade de São Paulo, CP 66318, São Paulo, SP 05314-970, Brazil

<sup>39</sup> George P. and Cynthia Woods Mitchell Institute for Fundamental Physics and Astronomy, Department of Physics and Astronomy, Texas A&M University, College Station, TX 77843, USA

<sup>40</sup> LPSC Grenoble - 52 Avenue des Martyrs, 3826 Grenoble, France

<sup>41</sup> Institució Catalana de Recerca i Estudis Avançats, E-08010 Barcelona, Spain

<sup>42</sup> Department of Astrophysical Sciences, Princeton University, Peyton Hall, Princeton, NJ 08544, USA

<sup>43</sup> Observatório Nacional, Rua Gal. José Cristino 77, Rio de Janeiro, RJ 20921-400, Brazil

<sup>44</sup> Department of Physics, Carnegie Mellon University, Pittsburgh, Pennsylvania 15212, USA

<sup>45</sup> Department of Physics and Astronomy, Pevensey Building, University of Sussex, Brighton, BN1 9QH, UK

<sup>46</sup> School of Physics and Astronomy, Southampton SO17 1BJ, UK

<sup>47</sup> Computer Science and Mathematics Division, Oak Ridge National Laboratory, Oak Ridge, TN 37831

<sup>48</sup> Department of Physics, Duke University Durham, NC 27708, USA

<sup>49</sup> Université Grenoble Alpes, CNRS, LPSC-IN2P3, 38000 Grenoble, France

<sup>50</sup> Department of Astronomy, University of California, Berkeley, 501 Evans Hall, Berkeley, CA 94720, USA

<sup>51</sup> Lawrence Berkeley National Laboratory, 1 Cyclotron Road, Berkeley, CA 94720, USA

This paper has been typeset from a TeX/LaTeX file prepared by the author.



You saw on the first page how many people contributed to this work and the Dark Energy Survey. This is (roughly) where every author's institution for this paper is!

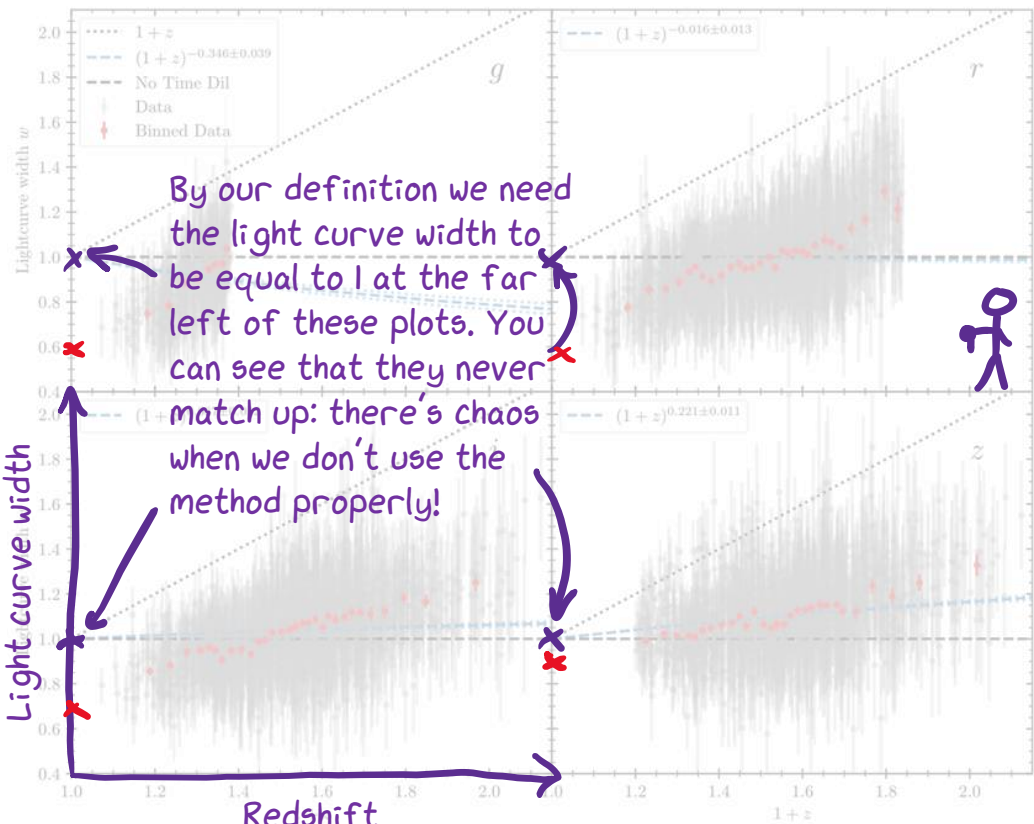


Figure C1. Light curve widths measured with respect to a reference curve that has *not* been de-time-dilated. We nevertheless still see a persistent trend of increasing light curve width with redshift. The vertical offset from the reference curve is because the non-de-time-dilated reference curves are wider than rest-frame light curves, i.e. this offset is yet another measure of the dilation. The black horizontal dashed line indicates no time dilation and the blue dashed lines are (poor)  $(1+z)^b$  model fits to the data. If there was no time dilation, these fits would be horizontal lines with  $b=0$ .

Congratulations on making it to the end! We've put a lot of effort into making the paper readable to astrophysicists, but I hope these notes were readable regardless of your background!

These scribbles were inspired by the wonderful work of [Claire Lamman](#) and [Sydney Vach](#) (who was also inspired by Claire!) Please go check out their annotated papers [here](#) and [here](#). I used PowerPoint to write over the paper text and plots by hand, using the XKCD font for the text (you don't want to see my handwriting!). You can download the font at [github.com/ipython/xkcd-font](https://github.com/ipython/xkcd-font)

Want to read more about the Dark Energy Survey? There's a lot of cool science happening! [darkenergysurvey.org](http://darkenergysurvey.org)

Ryan White, me!